

Energy Barriers in Magnetic Random Access Memory Elements

Rok Dittrich, Thomas Schrefl, Hermann Forster, Dieter Suess, Werner Scholz, and Josef Fidler

Abstract—Minimum energy paths and energy barriers are calculated for the free data layer in elliptical magnetic random access memory elements using a recently developed method that combines the nudged elastic band method with finite-element micromagnetics. The method calculates the magnetic states along the most probable reversal paths for applied fields below the zero temperature switching field. The reversal mode in the minimum energy path depends on the strength of the external field. With increasing easy axis field, the reversal mode becomes more inhomogeneous than at lower fields.

Index Terms—Energy barriers, magnetic random access memory (MRAM) elements, minimum energy path, nudged elastic band method (NEB), reversal modes, saddle points, thermal stability.

I. INTRODUCTION

WITH decreasing size of magnetic structures, thermal effects become even more important. In magnetic recording applications, spontaneous magnetization reversal by thermal agitation can lead to a loss of the recorded data. The energy barrier between stable configurations determines the probability of a thermal switching event. In magnetic random access memory (MRAM) elements, the energy barrier is determined by the shape of the element (shape anisotropy) and the induced crystalline anisotropy. This should guarantee a lifetime of a stored bit of about ten years. We calculate energy barriers for elliptical MRAM elements using the “nudged elastic band” method (NEB) [1]. This method finds minimum energy paths in high-dimensional energy landscapes and is a rigorous way to compute the saddle point(s) between local energy minima.

II. THEORY

Henkelman and Jónsson proposed the nudged elastic band method to calculate minimum energy paths and energy barriers [1]. The method is very robust and applicable when the energy landscape is smooth. This is mostly the case in micromagnetics. To calculate the minimum energy path between two local energy minima, an initial path is assumed (simple guess) between the states. The initial path is represented by a discrete sequence of images $M(k)$ and connects the initial magnetization state $M(i) = M(1)$ with the final magnetization state $M(f) = M(m)$. The index k runs from 1 to m . The path is

optimal, if for any image $M(k)$ the gradient of the energy is only pointing along the path. In other words, the component of the energy gradient normal to the path is zero. This path is called minimum energy path, which means that the energy is stationary for any degree of freedom perpendicular to the path. The minimum energy path typically represents the path with the greatest statistical weight. From this path, statistical quantities as for example transition rates for the thermally induced magnetization reversal can be estimated.

We use finite-element micromagnetics [2] to model the structures and to calculate energies, energy gradients, and effective magnetic fields. The minimum energy path is then found using an iterative scheme. In each step, the images move toward lower energy in a direction perpendicular to the path. This iterative scheme is numerically very ineffective. Instead, we solve a system of ordinary differential equations using the implicit ordinary differential equation solver CVODE [3]. Details on the implementation of the NEB method can be found in [1] and [4].

III. RESULTS

A. Model of the Free Data Layer

We constructed our models of the free layer of the MRAM based on an experimental work [5], which studies the thermal reversal of elliptical NiFeCo MRAM elements. Minimum energy paths (MEP) were calculated as a function of the external in plane field, below the zero temperature switching field. Material parameters of NiFeCo [6] were used ($J_s = 1.068$ T, $A = 10$ pJ/m, $K = 510$ J/m³) with the easy axis along the long axis of the element. We varied the size of the elements starting with an element of 1120×400 nm size and decreasing the size down to 62.5×25 nm. Aspect ratio (2 : 5) and thickness (4 nm) were kept constant. Fig. 1 shows a top view of the model with possible paths for the 1120-nm element.

1) *Reversal Modes at 1.12 μ m Size:* By varying the field strength along the easy axis, three minimum energy paths are found (Fig. 1) for a particle size of 1.12 μ m. Two of them show a single energy barrier where the magnetization reverses by inhomogeneous rotation in the film plane (path 1 and path 2 in Fig. 1). The third mode is a two-step reversal, which has a metastable state where a vortex is in the center of the element (path 3 in Fig. 1).

From a dynamic hysteresis calculations (integration of the Landau–Lifshitz–Gilbert equation using a Gilbert damping constant of $\alpha = 1$) [2], a zero temperature switching field of 94 Oe is found. The underlying reversal mode during the switching driven by an external easy-axis field larger than 94 Oe is similar

Manuscript received January 10, 2003. This work was supported by the Austrian Science Fund (Y-132 PHY).

The authors are with the Institute of Solid State Physics, Vienna University of Technology, 1040 Wien, Austria (e-mail: rok.dittrich@tuwien.ac.at).

Digital Object Identifier 10.1109/TMAG.2003.816239

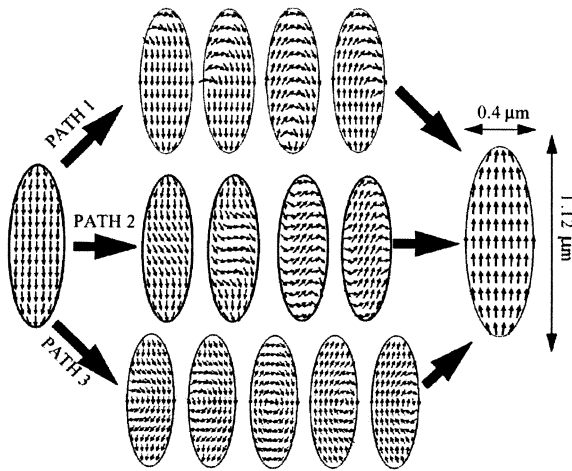


Fig. 1. Three minimum energy paths for the thermal reversal of a 4-nm thin NiFeCo MRAM element are found between the two stable states. An opposing field is applied along the easy axis (= long axis). In paths 1 and 2, the magnetization stays in plane crossing a single barrier. In path 3, a two-step reversal mode is found passing a metastable state (vortex in the center). For an applied field in the range 0–15 Oe, path 3 has the lowest barrier. From 15 to 80 Oe, path 1 has the lowest barrier and above 80 Oe, path 2 has the lowest barrier (see Fig. 2). The zero temperature switching field is 94 Oe.

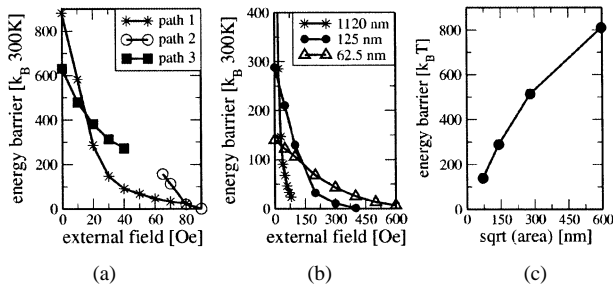


Fig. 2. (a) Energy barrier as a function of the easy-axis field strength for 1.12 μm particle size (see Fig. 1). The underlying thermal reversal mode (paths) depends on the strength of the external field. In paths 1 and 2, the magnetization stays in plane crossing a single barrier. In path 3, a two-step reversal mode is found passing a metastable state (vortex in the center). Above 15 Oe, path 1 has the lowest energy barrier (b). Energy barrier as a function of the easy-axis field strength for different particle size. (c) Energy barrier at zero external field as a function of the particle size (given in the square root of the top surface area). Thickness (4 nm) and aspect ratio (2:5) are fixed as in Fig. 1. The energy barrier depends close to linearly on the square root of the area of the MRAM element.

to the mode of path 2 in Fig. 1. This is in agreement with the following observation: At a field strength of $H < 15$ Oe, the mode of path 3 has the lowest barrier while for $H > 15$ Oe the mode of path 1 becomes favorable. Above 80 Oe, we are already close to the zero temperature switching field and the mode of path 2 becomes the mode with the smallest energy barrier. Fig. 2(a) shows the energy barriers of the three paths as a function of the applied field.

B. Variation of the Particle Size

Fig. 2(b) and (c) shows the size dependence of the energy barrier when an easy-axis field is applied. The extrapolation to the zero barrier height [Fig. 2(b)] gives a switching field value that agrees with the zero temperature switching field obtained with the dynamic calculation of the switching fields [Fig. 3(a)]. At

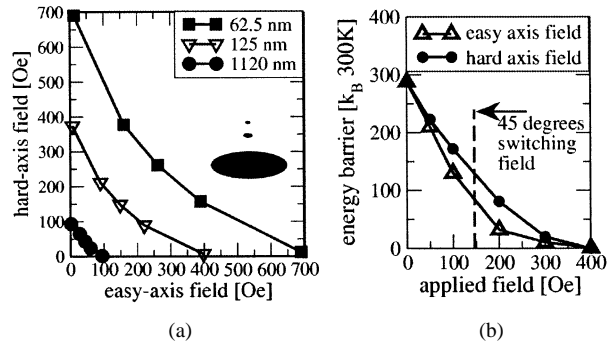


Fig. 3. (a) Switching astroid for three different sizes of a 4-nm thin elliptical MRAM element of aspect ratio 2:5. The given size is the length of the long axis. (b) Comparison of the energy barrier of a 125-nm element when applying either an easy-axis or a hard-axis field. Applying an easy-axis field is more critical for the stability than when applying a hard-axis field.

zero external field, the energy barrier depends almost linearly on the square root of the top surface area of the element [Fig. 2(c)].

C. Stability

From the switching astroid, we see that we obtain the lowest switching field when applying the field in plane at about 45° to the easy axis. At 1.12 μm size, this corresponds to a hard-axis and easy-axis field of 43 Oe. To ensure thermal stability, the MRAM must stay stable when applying either a hard- or a easy-axis field only of this strength. At a easy-axis field of 43 Oe, the energy barrier is $75 k_B 300$ K, which is high enough to ensure stability in the range of decades. For hard-axis fields, the situation was found to be less critical. Fig. 3(b) compares the energy barrier dependence on the external field for 125-nm particle size. The lowest switching field [Fig. 3(a)] is obtained at 45° with 148 Oe hard- and easy-axis field. The energy barrier is about $140 k_B 300$ K for a hard axis field of 148 Oe and $80 k_B 300$ K for an easy-axis field of 148 Oe [see Fig. 3(b)].

D. Field Dependence of the Reversal Mode

As shown earlier, the reversal modes found in the minimum energy paths depend on the field strength and direction of the applied field. For the large element, we found three paths as shown in Figs. 1 and 2(a). Even more surprising, we also see this for the smallest particle studied (62.5 nm). One would expect that the reversal mode would be close to homogenous rotation at this size. This is indeed the case when no field is applied. At stronger easy-axis fields, however (above 200 Oe), the mode changes to an inhomogeneous reversal involving a domain-wall motion similar to the mode of path 1 in Fig. 1, but now with the wall oriented along the short axis (Fig. 4). Fig. 5(a) shows the energy along the minimum energy paths for the 62.5-nm element as a function of the arclength. The energy is normalized to the energy of the initial (nonreversed) state. Different easy-axis fields are applied. The change of the reversal mode is also observed in the increase of the arclength of the path above 200 Oe. The mode has become more inhomogeneous, which is seen in Fig. 4. As a consequence, the total length of the path increased.

The field dependence of the reversal mode found is explained as follows: at low external fields, the reversal mode is mainly determined by the competition of exchange and stray-field energy. At higher fields, the Zeeman energy has a stronger weight

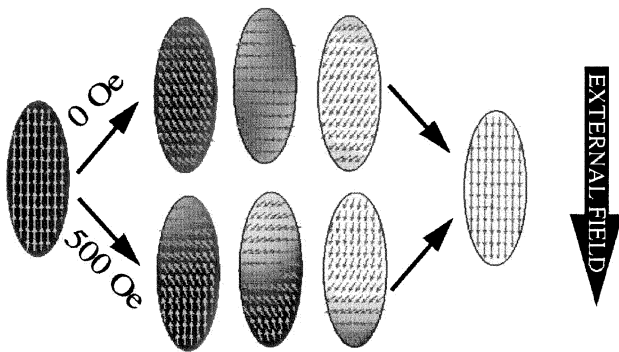


Fig. 4. Minimum energy paths for the thermal reversal of a 4-nm thin NiFeCo MRAM element of 62.5 nm size. An opposing field is applied along the easy axis (= long axis). Black: magnetization “up.” White: magnetization “down.” For fields stronger than 100 Oe, there is an abrupt change of the reversal mode to the one shown here (500 Oe).

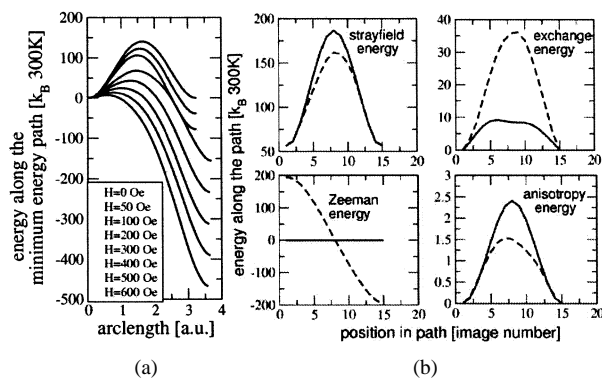


Fig. 5. (a) Energy along the minimum energy paths for a 62.5-nm element as a function of the arclength in the path. The energy is normalized to the energy of the initial (nonreversed) state. Different easy-axis fields are applied. The increase of the length of the path above 200 Oe is due to a change of the reversal mode. The mode has become more inhomogeneous, which is seen in Fig. 4 and Fig. 5(b). (b) Energies along the minimum energy path for a 62.5-nm element. The solid line shows energies when no field is applied. The dashed line is for an applied easy-axis field of 500 Oe. The exchange energy is four times higher than at no applied field. This reflects the more inhomogeneous reversal mode.

and it can get an advantage to follow a more inhomogeneous mode. More energy is “spent” in exchange, but therefore more energy is gained in the Zeeman part. In total, the energy barrier is smaller even though the mode has become more complex. This observation is shown in Fig. 5(b). The four energy contributions along the minimum energy paths are compared for 62.5-nm par-

ticle size. We compare the path obtained with zero external field with a path obtained for $H = 500$ Oe. The exchange energy is four times higher at 500 Oe than at zero field since there is a domain-wall motion involved here. The anisotropy energy only plays a minor role, which means that the shape of the particle and the external field dominates the behavior of the reversal mode and height of the energy barrier.

For hard-axis fields, the opposite behavior is observed. The reversal mode becomes more homogenous at stronger fields.

IV. CONCLUSION

Energy barriers and minimum energy paths in elliptical MRAM elements were calculated using the nudged elastic band method. We found that more than one minimum energy path can exist. The reversal mode depends on the strength and direction of the applied field. With increasing easy-axis field, the mode becomes more inhomogeneous while the opposite is the case for hard-axis fields. Varying the sizes of the element, we find that the energy barrier increases about linearly with the square root of the top surface area.

ACKNOWLEDGMENT

The authors thank A. Thiaville and J. Miltat for helpful discussions.

REFERENCES

- [1] G. Henkelman, B. P. Uberuaga, and H. Jónsson, “Improved tangent estimate in the NEB method for finding minimum energy paths,” *J. Chem. Phys.*, vol. 113, p. 9901, 2000.
- [2] D. Suess, V. Tsiantos, T. Schrefl, J. Fidler, W. Scholz, H. Forster, R. Dittrich, and J. Miles, “Time resolved micromagnetics using a preconditioned time integration method,” *J. Magn. Magn. Mater.*, vol. 248, p. 298, 2002.
- [3] S. D. Cohen and A. C. Hindmarsh, “CVODE, A stiff/nonstiff ODE solver in C,” *Comput. Phys.*, vol. 10, p. 138, 1996.
- [4] R. Dittrich, T. Schrefl, D. Suess, W. Scholz, H. Forster, and J. Fidler, “A path method for finding energy barriers and minimum energy paths in complex micromagnetic systems,” *J. Magn. Magn. Mater.*, vol. 250, p. 12, 2002.
- [5] N. D. Rizzo, M. DeHerrera, J. Janesky, B. Engel, J. Slaughter, and S. Tehrani, “Thermally activated magnetization reversal in submicron magnetic tunnel junctions for magnetoresistive random access memory,” *Appl. Phys. Lett.*, vol. 80, p. 2335, 2002.
- [6] S. Ingvarsson, G. Xiao, S. S. P. Parkin, and W. J. Gallagher, “Thickness-dependent magnetic properties of $\text{Ni}_{81}\text{Fe}_{19}$, $\text{Co}_{90}\text{Fe}_{10}$ and $\text{Ni}_{65}\text{Fe}_{15}\text{Co}_{20}$ thin films,” *J. Magn. Magn. Mater.*, vol. 251, p. 202, 2002.